ELSEVIER

Precambrian Research 116 (2002) 183–198

Precambrian Research

www.elsevier.com/locate/precamres

B–Na rich Palaeoproterozoic Aravalli metasediments of evaporitic association, NW India: a new repository of gold mineralization

P.R. Golani [a], M.K. Pandit [b,*], A.N. Sial [c], A.E. Fallick [d], V.P. Ferreira [c], A.B. Roy [e]

[a] *P.No. 181, Sindhi Colony, Bani Park, Jaipur 302 016, India*
[b] *Department of Geology, University of Rajasthan, Jaipur 302 004, India*
[c] *Department of Geology, Center for Technology and Geosciences, NEG LABISE, UFPE, C.P. 7852 Recife PE 50 732-970, Brazil*
[d] *Scottish Universities Environmental Research Center, East Kilbride, Glasgow G75 0QF, Scotland, UK*
[e] *Paneriyon ki Madari, Hiran Magari, Udaipur 313 002, India*

Received 30 March 2000; accepted 31 January 2002

Abstract

We report field observations and preliminary petrochemical and stable isotopic compositions of the host rock and sulfide minerals for a recently discovered sulfide-hosted gold deposit from the Palaeoproterozoic Aravalli rocks in northwestern India. Gold occurs associated with Fe–As–Cu ($\pm$Co) sulfides in lithofacies of diverse mineralogical composition, dominated by amphibole-bearing dolomitic marble and albite-rich quartzo-feldspathic rocks (QFR). The presence of vugs, believed to be after dissolution of halite patches, coupled with the development of scapolite-bearing assemblages in dolomite marble, occurrence of tourmaline-rich mineralized rocks and very high Na content of carbonates and QFR indicate hypersaline depositional environment for the host rock. A narrow spread of $\delta^{34}S_{CDT}$ values from +10.5 to +12.8‰ for stratiform arsenopyrite and remobilized pyrrhotite, corroborates hypersaline to evaporitic depositional environment. The $\delta^{13}C$ values for gold-bearing carbonates show bimodal distribution; one population (mean $-0.4‰_{V\text{-}PDB}$) is close to the sea water carbonate values while the other ($-3.1‰$) indicates probable mantle affinity. The $\delta^{18}O$ values for carbonates (mean $= +18.4‰_{V\text{-}SMOW}$) are not discriminative as they appear to have been modified by subsequent metamorphism and hydrothermal activity. Interpretation of mantellic source for carbon is borne out from the absence of biogenic activity and incompatibility of significantly negative $\delta^{13}C$ values in the evaporitic setting of deposition of Bhukia rocks. We suggest that Na–B rich fluids, channeled through rift-related faults, were responsible for creating hypersaline conditions that eventually evolved into an evaporitic environment. Mantle carbon, through some still deeper faults, was probably responsible for the gold transport and its subsequent deposition in an otherwise uncommon (evaporitic) repository of carbonates and QFR. © 2002 Elsevier Science B.V. All rights reserved.

Keywords: Palaeoproterozoic evaporite; Aravalli Supergroup; C–O, S isotopes; Gold-sulfide mineralization, NW India

* Corresponding author. Tel.: +91-141-514793.
E-mail address: mpandit_jp1@sancharnet.in (M.K. Pandit).

0301-9268/02/$ - see front matter © 2002 Elsevier Science B.V. All rights reserved.
PII: S0301-9268(02)00020-7

1. Introduction

Palaeoproterozoic rocks of Aravalli Supergroup, in northwestern India (Fig. 1) represent shallow-water depositional environments, interpreted as epicontinental seas (Roy and Paliwal, 1981), except in the western part of the basin. Initiated by outpouring of rift-related basic volcanic lavas (with minor orthoquartzite) over a dominantly granitic Archaean basement, the

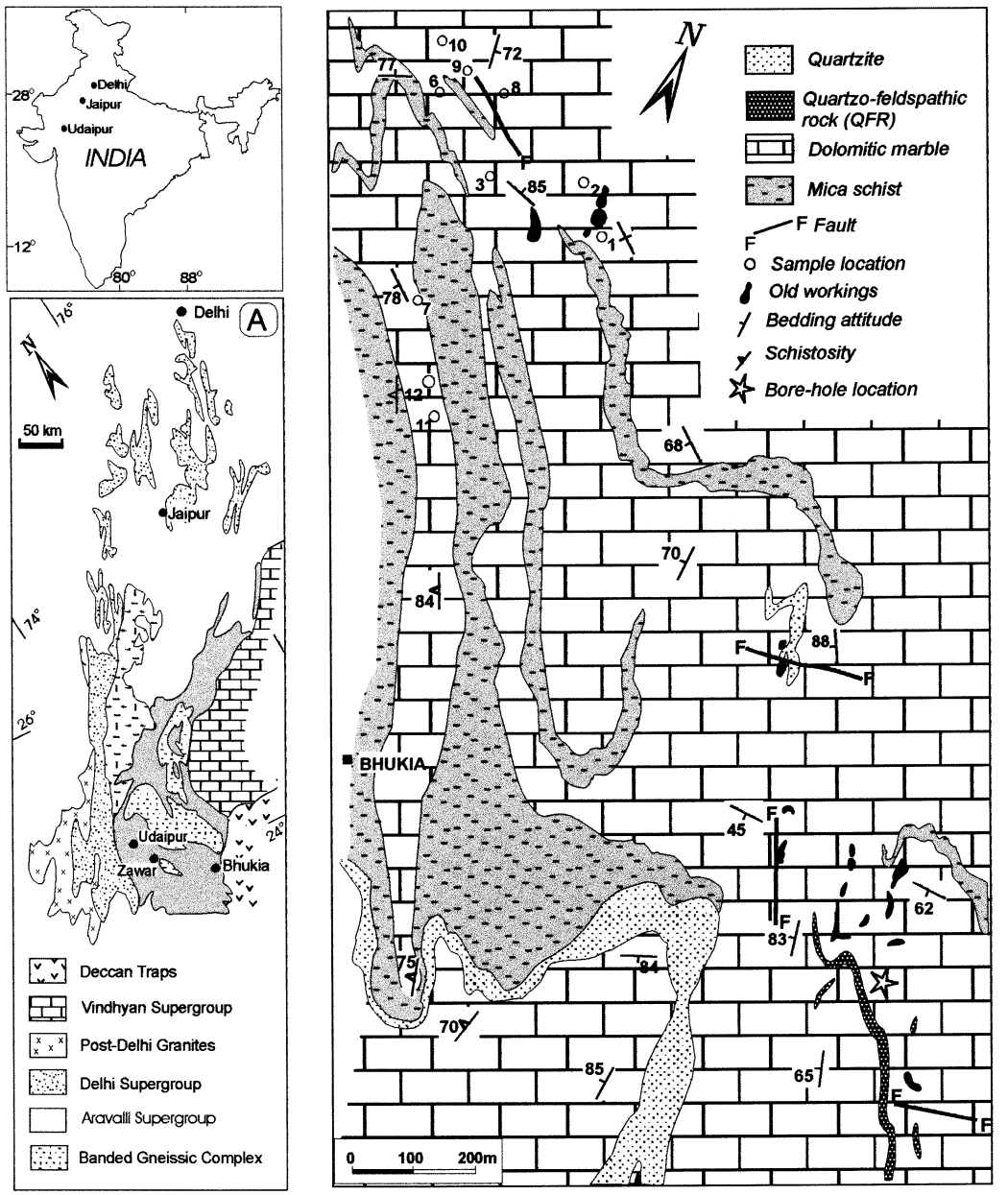

Fig. 1. Geological map of Bhukia area showing location of samples analyzed for whole rock chemistry, Sulfur-isotopes and location of bore-hole (illustrated in Fig. 4). A. Simplified geological map of the Aravalli Mountain Range, NW India showing major stratigraphic units and location of the Bhukia Gold Prospect.

Aravalli sedimentation is characterized by depositional conditions conducive for prolific growth of phosphate-bearing stromatolites in dolomites with localized attainment of euxinic settings, leading to the development of carbonaceous sediments. The shallow-water nature of the depositional environment remained significant during deposition of quartzite and carbonates of younger Aravalli formations. The end phase of Aravalli sedimentation is represented by siltstones, deposited in fluviatile environments (Paliwal, 1998). However, while working on the recently discovered gold mineralization in Bhukia area in southeastern Rajasthan (Grover and Verma, 1993), we have noted evidence of evaporitic depositional environment, hitherto unrecognized in the Aravalli Supergroup and also an uncommon repository for gold-sulfide mineralization. The significance of brine and evaporitic association is being increasingly realized in deposition of base metals such as the Copper Belt of Central Africa (Moine et al., 1981) and the metalliferrous Proterozoic Willyama Supergroup of Australia (Cook and Ashley, 1992). However, nowhere is gold mineralization reported from these hypersaline environments. This paper presents field observations and petrological details on this atypical geological setting of the Bhukia gold mineralization. Hydrothermal features and stable isotopic compositions presented here have been interpreted, taking cognizance of the geological data, for this newly discovered gold-evaporite association.

2. Geological setting

The Precambrian terrane of Rajasthan in nortwestern India exposes several geological sequences comprising the successively younger Proterozoic tectonostratigraphic units; the Aravalli and Delhi Supergroups that overlie a dominantly sialic Archaean basement (BGC of Heron, 1953). The sialic basement in southeastern Rajasthan is represented by a gneiss—metasediment—amphibolite sequence which shows pristine Archaean character (Mewar Gneiss Complex of Roy and Kröner, 1996), Late Archaean granitoids (Wiedenbeck et al., 1996) and part of the gneiss—granulite terrane which had undergone tectonothermal reconstitution during the Proterozoic. Geochronological data indicate that Archaean rocks have an evolutionary history spanning a period of more than a billion years from $\sim$3500 to 2500 Ma (Vinogradov et al. 1964; Gopalan et al. 1990; Roy and Kröner, 1996; Wiedenbeck et al. 1996).

Heron's (1953) recognition of a profound erosional unconformity between the Archaean basement and the oldest cover unit, the Aravalli Supergroup, has been confirmed by subsequent studies in the region to the east and southeast of Udaipur (Roy and Paliwal, 1981 Naha and Roy, 1983; Roy et al., 1988). A Palaeoproterozoic age of approximately 2.15 Ga for the Aravalli Supergroup is suggested by Pb-isotope dating of galena associated with barite bands within the basal mafic volcanic sequence at Negaria, north of Udaipur (M. Deb and R. Thorpe, personal communication, see also Roy and Kataria, 1999). Model Sm–Nd ages of the basal metavolcanics in the type area around Udaipur range between 2.6 and 2.3 Ga (Macdougall et al., 1984). Other than these volcanics, the Aravalli rocks of the shelf sequence comprise a shale–sand–carbonate assemblage (the latter being represented by dolomitic marble and crystalline limestone) and a dominant mica schist unit with subordinate quartzite. Greywacke occurs in significant proportion in the Udaipur valley. In the type section around Udaipur, the carbonate rocks mainly occur at three stratigraphic levels (Fig. 2A). The Aravalli rocks show polyphase deformation and metamorphic history. The deformation pattern is more complex in the southern belt, which also includes Bhukia Gold Prospect, due to superimposition of younger (possibly Neoproterozoic) deformation. The grade of metamorphism in the Aravalli rocks in the type section around Udaipur is generally low; however, there are high-grade zones in the southeastern and western parts of the Aravalli Fold Belt, close to the tectonic contact with the Delhi Supergroup. The patchy distribution of high-grade metamorphism due to local increase in metamorphic grade can be attributed

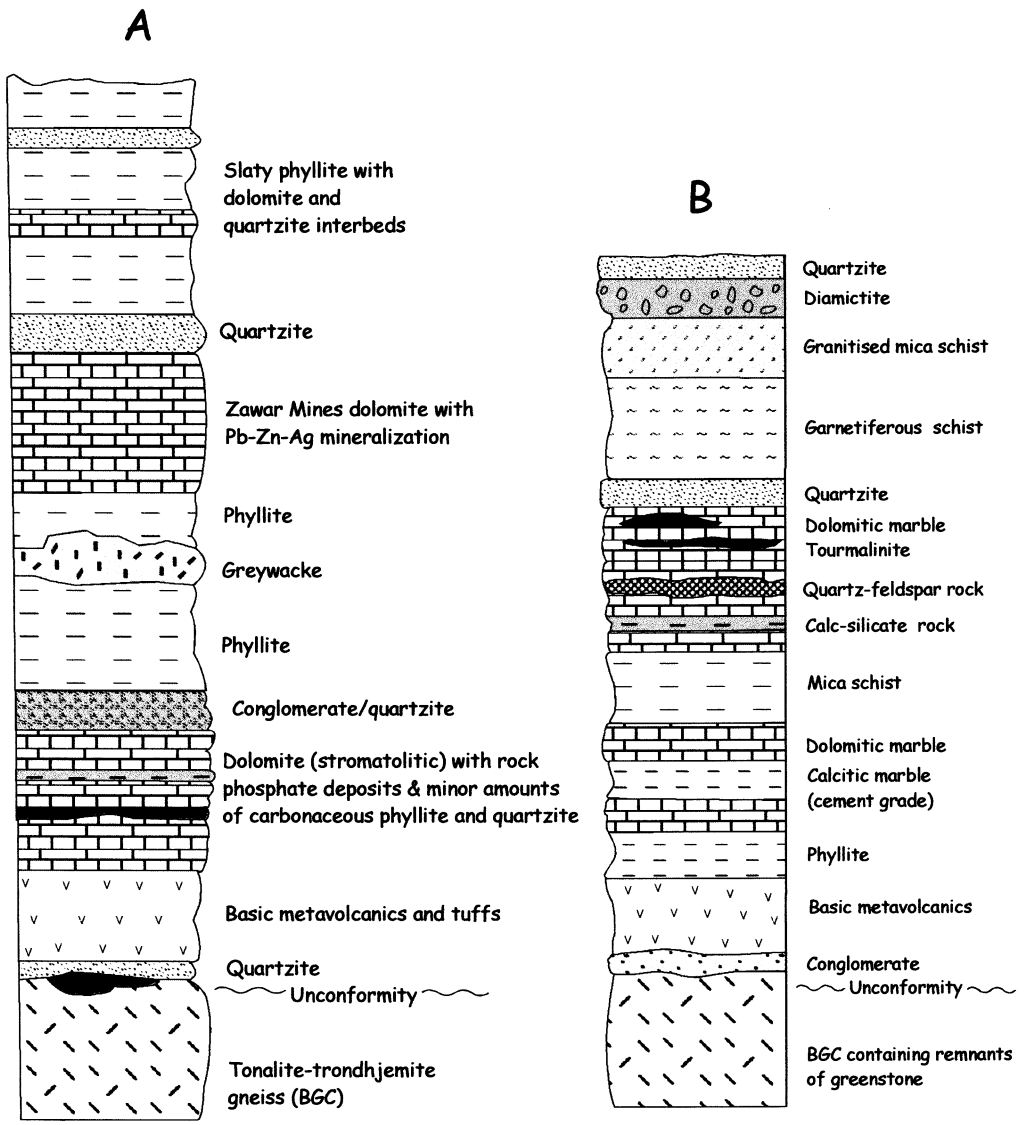

Fig. 2. Summary stratigraphy of the Aravalli Supergroup in Southeastern Rajasthan. (A) Stratigraphic sequence of the type area around Udaipur (Zawar), mainly after Roy et al. (1988). (B) Lithostratigraphic section of Bhukia area showing position of host rocks of gold and sulfide mineralization.

to younger (post-Aravalli) thermal perturbations. The older, dolomitic marble unit occurring at Jhamarkotra (20 km SE of Udaipur) hosts stromatolitic rock phosphate. The younger, dolomitic succession is represented by Zawar Mines sequence, which hosts Pb–Zn–Ag ore bodies. The present study focuses on the southeastern extension of the type section of Udaipur region (Fig. 1). In contrast to the Pb–Zn–Ag bearing upper carbonates of the type area, the Bhukia dolomitic marble and associated quartzofeldspathic facies host Fe–As–Cu ($\pm$Co) and gold. Zn is locally present in very small amounts and Pb and Ag are virtually absent. Fig. 2B gives a summary stratigraphic succession across the Bhukia Gold Prospect.

3. Host rock lithology

3.1. Carbonate rocks

The carbonate rocks, hosting the gold mineralization in the Bhukia area, include dolomitic marble, dolostone, amphibole marble and calc-silicate rocks, the latter grading into para-amphibolite. Calcitic marble is rare. Megascopically, the marble is medium- to coarsegrained and spotted with needles of tremolite and actinolite. A variant of dolomitic marble shows conspicuous cavities and elliptical pits. We refer this light to dark brown, medium- to fine-grained rock as 'pitted' dolomitic marble. Petrographically, the carbonates are recrystallized and medium- to coarse-grained. A few well-rounded, polycrystalline aggregates of quartz have been observed in some recrystallized calcitic marbles. The common mineral assemblages of carbonates are:

Dolomite ± calcite ± scapolite ± biotite ± plagioclase + quartz + opaques + titanite + tourmaline + apatite.

Ferroan calcite + well-rounded polycrystalline quartz ± hornblende + albite ± opaques

Dolomite + tremolite ± actinolite ± diopside + quartz ± feldspar ± talc ± titanite.

Lower abundances of SiO_2, MnO and P_2O_5 in dolomitic rocks (Table 1) discriminate them from the phosphate-bearing calcitic carbonates of Udaipur area that have relatively higher SiO_2, MnO and P_2O_5 concentrations (Banerjee, 1971). The Fe_2O_3/FeO ratio is usually > 1, suggesting extremely shallow depositional conditions and intermittent sub-aerial exposures. Likewise, the Na_2O/K_2O ratio is also very high. The Na concentration ranges between 1026 and 12 094 ppm with a mean of 5013 ppm. Barring the calc-silicate rocks, the K content of carbonates is very low, ranging from 165 to 3138 ppm, with a mean value of 972 ppm.

3.2. Quartzo-feldspathic rock

There are well-laminated thin bands of albite-rich quartzo-feldspathic rock (QFR) within the carbonates. In addition, fine QFR layers also occur inextricably mixed up with amphibole-bearing dolomite marble and calc-silicate rocks. Though widely present, the QFR rarely forms a mappable unit of its own (Fig. 1). The QFR is generally a fine-grained rock with local attainment of medium-grained texture. It shows heterogeneous mineralogical composition with extreme enrichment in albitic plagioclase (> 50%), mineralogically comparable to albitites. The quartz content is also variable. Calcite is noted as rare discrete grains along the boundary of albite

Table 1
Partial whole rock composition and C–O isotopic ratios of representative samples of Bhukia carbonates

Sample number	BJR1	BJR2	BJR3	BJR6	BJR7	BJR 8	BJR9	BJR10	BJR11	BJR12
Serial number	1	2	3	4	5	6	7	8	9	10
SiO_2 (wt.%)	4.17	4.36	4.90	22.99	5.20	4.17	18.18	2.08	38.42	11.63
$A12O_3$	1.03	0.29	1.47	0.88	0.88	1.03	3.53	0.44	9.20	1.76
Fe_2O_3	1.84	1.02	1.41	2.38	0.99	0.29	1.19	0.77	3.32	2.69
FeO	0.90	1.44	0.72	1.08	0.36	0.72	0.90	0.72	7.20	0.54
MgO	15.6	18.8	11.60	11.20	0.62	20.20	19.84	19.04	4.62	0.40
CaO	33.04	28.0	37.52	27.44	50.5	29.19	23.10	30.04	21.24	45.26
Na_2O	0.14	0.62	0.93	0.16	0.62	0.16	0.95	0.63	0.98	1.65
K_2O	0.03	0.02	0.03	0.06	0.26	0.07	0.12	0.09	2.20	0.38
LOI	43.26	44.92	40.85	33.67	40.15	44.28	31.53	45.25	11.74	35.08
Na/K	4.14	27.54	27.49	2.37	2.12	2.03	7.02	6.21	0.39	3.85
δ^{13} C‰$_{V\text{-}PDB}$	−1.5	−0.4	−4.1	−0.5	−3.0	+0.3	−0.9	−0.3	−3.3	−3.7
δ^{18}O‰$_{V\text{-}SMOW}$	+21.5	+21.4	+26.0	+19.7	+23.6	+21.8	+20.5	+20.0	+16.1	+15.3

1–3, dolomitic marble; 4, tremolite bearing dolomitic marble; 5, calcitic marble; 6–8, dolostone; 9, calc-silicate rock; 10, calcite marble.

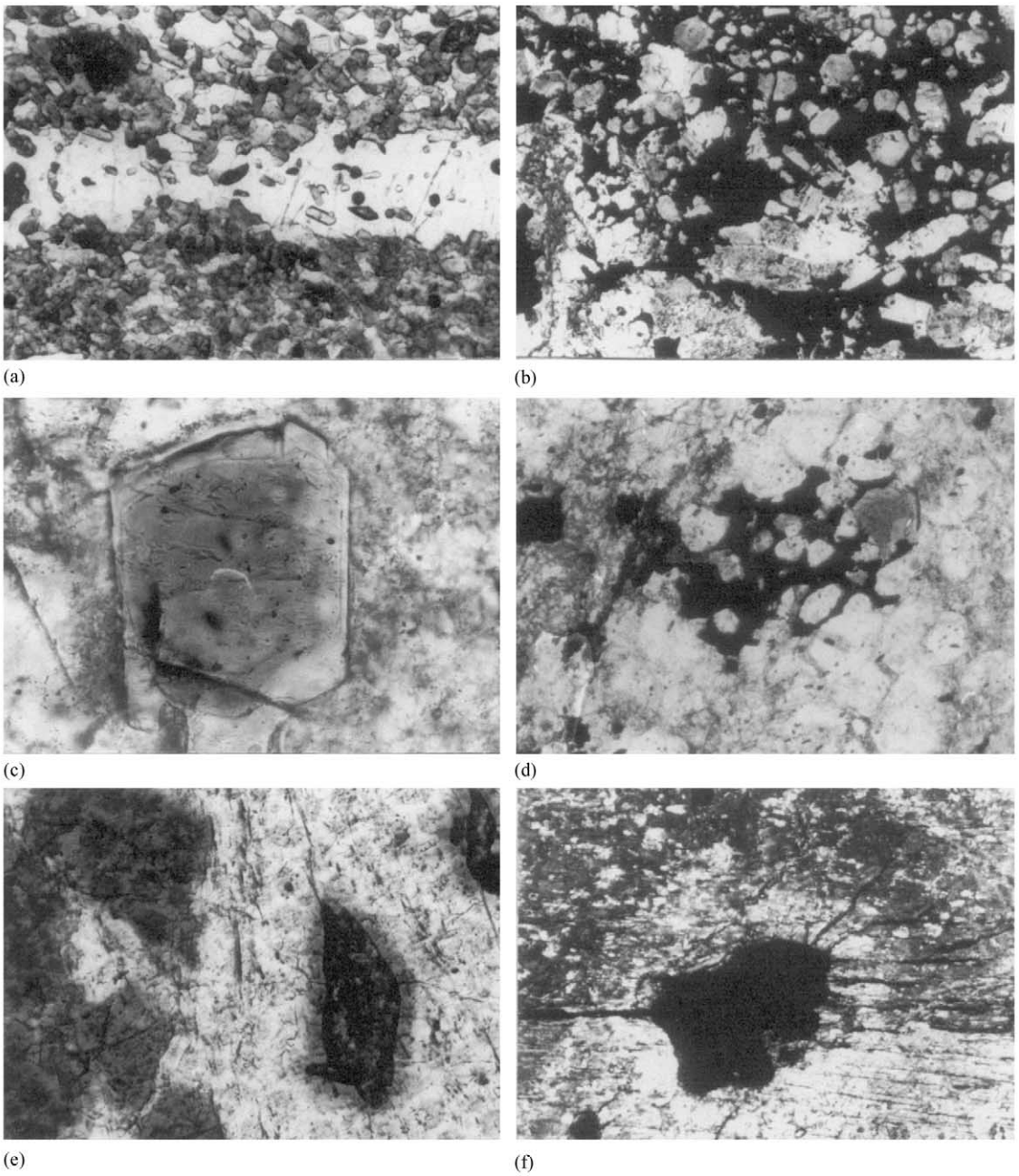

Fig. 3. Petrographic attributes of rocks of Bhukia Gold Prospect. (3a) Photomicrograph (PPL) showing tourmaline and quartz (Q) layering in tourmalinite. Longer dimension of photograph measures 2 mm. (3b) Photomicrograph (PPL) showing tourmaline–sulfide (pyrrhotite) association in Bhukia Gold Deposit. Longer dimension of photograph measures 2 mm. (3c) Dark (core) and light (rim) brown zoning in tourmaline (PPL). Longer dimension of photograph measures 0.8 mm. (3d) Composite grain of opaque and feldspar in QFR (PPL). Longer dimension of photograph measures 2 mm. (3e) Titanite in quartz rich layer in tourmalinite showing radioactive halo (PPL). Longer dimension of the photograph measures 0.4 mm. (3f) Radioactive opaque mineral with 'nimbus' and radial fractures in amphibole in partially polarized light. Longer dimension of photograph measures 2 mm.

grains. In addition, hair-thin calcite veins are also observed in the QFR. A noteworthy feature of the QFR is the ubiquitous presence of minor amounts of tourmaline. The tourmaline is pleochroic in shades of brown, similar to that observed in tourmaline-rich rocks. The sedimentary-nature of the albite-bearing QFR of Bhukia is borne out by the following pieces of evidence:

1. Alternately layered QFR, carbonates and tourmaline-rich rocks, and lack of any intrusive relationship.
2. Variation in the abundances of different minerals also preclude a magmatic origin as rocks crystallizing from a melt would usually show a higher degree of compositional uniformity (cf. Leake and Singh, 1986).
3. Schwartz (1992) has shown that albites crystallizing from hydrothermal fluids effecting metasomatism, incorporate considerable Ca in their composition. In contrast, the albites of Bhukia QFR are near pure end members (see Table 1) which appear consistent with Kastner and Siever (1979) findings on low-temperature sedimentary authigenic feldspars.

3.3. Tourmaline-rich rock

Thinly-laminated, tourmaline-rich rocks occur in association with QFR and sulfide mineralization in the southeastern part of the area (Fig. 1c). Tourmaline, at places, forms 1–5 mm thick layers which alternate with quartz, feldspar and chlorite-biotite rich layers (Fig. 3a). The tourmaline-rich bands contain as much as 55% modal tourmaline. Tourmaline also occurs closely associated with sulfides (Fig. 3b). Some of the larger grains show dark brown core and light brown rims (Fig. 3c). Petrographic examination shows opaque, cemented, composite clasts of tourmaline and feldspar in QFR (Fig. 3d). Solitary tourmaline grains also occupy interstitial spaces in QFR. A few grains of titanite, epidote and opaques in tourmaline rich rocks appear charged with radioactive elements, evident from development of radial cracks and 'nimbus' around minerals (Fig. 3e and f). The maximum coexisting mineral assemblage in tourmaline-rich rock (tourmalinite) is as follows:

Tourmaline + quartz + plagioclase ± epidote + chlorite + biotite + calcite + titanite + opaques (sulfides)

Besides a considerable degree of uniformity in composition of the tourmaline (Table 2), the mineral chemistry also reveals that:

1. Mg content is higher and average Na_2O contents of three samples are 2.42, 1.92 and 2.04%; Fe/Al ratio is significantly lower, ranging between 0.11 and 0.22 with a mean of 0.15;
2. TiO_2 content is high, ranging between 1.16 and 3.23% with a mean of 1.94%, and
3. the dark and light brown zones within individual grains are similar in chemical composition and do not show any pattern between core and rim in respect of Na, Mn, Si, Mg, Fe, Ca, K, Al, Cr, Ti and Ni.

The chemical composition of Bhukia tourmalines is plotted on the Al–Fe–Mg diagram (Fig. 4). The diagram shows that two samples plot close to the field of dravite, just below the schorl-dravite line while the third is located close to the schorl-dravite field (Henry and Guidotti, 1985). Some of the spot probe analyses of the Bhukia tourmaline closely compare with the evaporitic tourmalines reported from Liaoning in China (see Jiang et al., 1997). On the other hand they are well-discriminated from the metasomatic tourmalines (see Fiermans and Paepe, 1982).

A summary of the field, petrographic and geochemical characteristics, given below, suggests a hypersaline evaporitic depositional environment for the host carbonate and the associated facies.

1. Presence of 'pits' in the dolomitic marble, and Na content (mean 5013) significantly higher than the 1000–3000 ppm range for hypersaline and evaporitic (sabkha) environments and much above the 1000 ppm level reported for normal marine sedimentary carbonates (Neudert and Russell, 1981; Land and Hoops, 1973). High Na/K ratio of Bhukia rocks (Table 1) is comparable to some of the large soda lakes of the world (Kemp and Degens, 1985). High Na content is also a characteristic feature of the QFR. The possibility of soda metasomatism in the carbonate-QFR (± tourmalinite) litho-association is ruled out on the strength of well-bedded nature of lithounits, consistent pref-

Table 2
Microprobe analysis of representative tourmaline, mica and albite from Bhukia rocks

	Tourmaline												
wt.%	44/125	44/126	44/127	44/128	44/129	27/1	27/7	27/8	27/10	30/8R	30/9C	30/11C	30/12R
SiO_2	37.80	37.57	37.79	37.56	37.73	37.58	37.36	37.20	36.82	36.49	37.43	36.76	36.72
TiO_2	1.63	1.66	2.07	2.05	2.01	2.10	1.90	2.28	1.75	2.90	2.60	1.16	3.23
Al_2O_3	30.0	30.07	29.27	29.38	29.57	28.47	29.24	29.34	28.86	27.83	28.75	30.80	27.69
Cr_2O_3	–	–	–	–	–	0.00	0.04	0.00	0.06	0.25	0.10	0.12	0.13
FeO	3.74	3.34	3.31	3.43	3.46	3.03	3.11	3.20	4.30	5.06	4.58	7.10	5.56
MnO	0.00	0.09	0.03	0.14	0.02	0.00	0.00	0.00	0.03	0.01	0.03	0.00	0.00
MgO	10.67	10.25	11.23	10.62	10.71	11.20	10.81	10.68	10.19	9.76	11.09	7.95	9.67
BaO	0.48	0.00	0.08	0.00	0.00	n.d.	n.d.	n.d.	n.d.	n.d.	n.d.	n.d.	n.d.
CaO	1.86	1.72	2.5	1.95	1.87	2.16	1.92	1.92	2.25	1.61	1.50	0.80	1.67
Na_2O	2.13	2.24	1.67	2.10	2.07	1.94	2.03	1.97	1.74	2.17	2.65	2.73	2.12
K_2O	0.04	0.02	0.04	0.05	0.02	0.02	0.03	0.03	0.02	0.04	0.00	0.00	0.01
P_2O_5	0.10	0.04	0.00	0.00	0.00	0.00	0.50	0.14	0.03	0.00	0.00	0.00	0.00
Cl	0.01	0.00	0.02	0.00	0.00	n.d.	n.d	n.d	n.d	–	–	–	–
F	0.08	0.09	0.03	0.03	0.02	n.d.	n.d	n.d	n.d	–	–	–	–
	Phlogopite			Albite									
	44/137	44/138	30/10	30/7	162/2	162/6	162/12	162/18	181/20	45/1	45/2	45/4	45/7
SiO_2	40.93	40.15	41.21	67.08	68.20	68.26	69.12	68.67	68.42	68.89	66.89	68.68	69.19
TiO_2	0.98	0.83	0.99	3.71	0.01	0.00	0.16	0.01	0.09	0.00	0.00	0.00	0.05
Al_2O_3	15.23	15.48	14.34	19.45	19.52	19.60	19.77	19.60	20.03	19.49	19.16	19.80	19.65
FeO	7.54	7.68	10.04	0.08	0.06	0.04	0.75	0.03	0.00	0.01	0.72	1.05	0.07
MnO	0.00	0.08	0.20	0.00	0.00	0.00	0.00	0.00	0.00	0.00	0.00	0.00	0.00
MgO	21.45	21.01	20.27	0.04	0.00	0.01	0.03	0.03	0.05	0.01	0.00	0.00	0.04
BaO	0.07	0.22	n.d.	–	–	–	–	–	–	–	–	–	–
CaO	0.00	0.12	0.10	0.14	0.56	0.13	0.15	0.16	0.30	0.01	0.11	0.22	0.03
Na_2O	0.15	0.21	0.21	11.43	11.61	11.58	11.84	11.55	11.84	11.36	11.23	11.65	11.72
K_2O	10.10	9.85	8.64	0.00	0.04	0.00	0.02	0.00	0.05	0.04	0.08	0.06	0.05
P_2O_5	0.04	0.00	0.05	0.02	–	–	–	–	–	–	–	–	–

n.d., not determined.

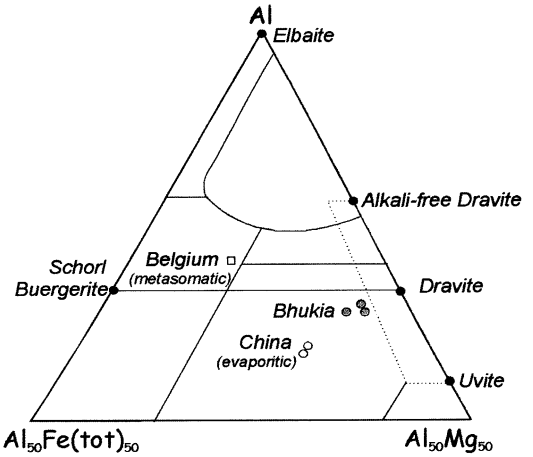

Fig. 4. The Al–Fe–Mg (molecular proportions) plot, after Henry and Guidotti (1985), for tourmaline of Bhukia area. Note a close similarity of Bhukia tourmalines with evaporitic tourmalines from Liaoning, China (Jiang et al., 1997), both well-discriminated from the metasomatic tourmalines from Belgium (Fiermans and Paepe, 1982).

erence of Na throughout the deposition of host-rock litho-association and purity of albites, all considered to be diagnostic of sedimentary feldspars (Kastner and Siever, 1979).

2. Mineral analyses of brown biotite, a common mineral in the Bhukia Gold Prospect rocks, reveal that it is phlogopitic in composition (Table 2). Phlogopite has been cited as an important index mineral in most of the meta-evaporitic sequences (Moine et al., 1981).
3. Development of scapolite-bearing assemblages in Bhukia carbonates indicate evaporitic affinity (cf. Serdyuchenko, 1975).
4. Presence of tourmaline and its common occurrence as disseminations in the quartzo-feldspathic facies as well as thin tourmalinite bands indicate high boron flux in the depositional environment. Such assemblages are reported from meta-evaporites of China (Peng and Palmer, 1995) and Australia (Cook and Ashley, 1992). Extremely low Fe/Al ratio (mean 0.15) in Bhukia tourmalines is far below the 38.51 level (range 10.5–62.22), reported for submarine hydrothermal deposits (Von Damm et al., 1985). On the other hand, the closest analogues are the tourmalines reported from the Proterozoic meta-evaporitic sequences of China (Jiang et al., 1997) whose Fe/Al ratio ranges from 0.29 to 0.87 (mean 0.48).

4. Gold-sulfide mineralization

Gold-sulfide mineralization is hosted by dolomitic marble, QFR and its variants, exposed near Bhukia, about 75 km southeast of Udaipur in NW India (Fig. 1). Gold occurs as microscopic grains (20–30 μm), generally in association with arsenopyrite and lollingite. Chalcopyrite is a less favored repository of gold while pyrrhotite-rich assemblages, despite being the most dominant in sulfide phase, rarely give significant gold values. Bi, Te, Co and Ni occur in minor amounts in gold-rich arsenopyrite and lollingite. Ag is invariably in traces. Virtual absence of Pb and Zn sulfides is a very significant feature. Pyrite is rare and confined mainly to the central part of the prospect. Titanite and ilmenite are other minerals associated with sulfidic assemblages. Uncommon minerals include native bismuth, alloys of Au and Bi (maldonite) and Bi–Te (wehrlite), reported by Golani et al. (1999).

Megascopically the sulfide minerals form bands and stringers. There are also disseminated specks, fracture fillings and patches of sulfide in host rock. Massive sulfides are invariably pyrrhotite-dominated, generally forming ore breccia, typically with fragments of quartz and albitic feldspar. Tourmaline also occupies interstitial spaces in the breccia. Sulfide fragments with rounded gangue also occur as rip-off components in the QFR. On a larger scale, the sulfide-gold mineralization is layer parallel to the enclosing impure dolomite marble, and its facies variants. On hand specimen scale, some core cuttings show clear relationship between finely-laminated tourmalinite, QFR and arsenopyrite. The arsenopyrite occurs as laminae-parallel pods and lenticles along the interphase of tourmalinite and QFR. Arsenopyrite and tourmaline also occur as discrete grains and clusters, parallel to layering, within the QFR bands (Fig. 5). The tourmaline-QFR interlayers are sometimes displaced by

small-scale horst and graben-like faults at high angle to the layering. At several places the microfaults and fractures are occupied by carbonate veins (Fig. 5). In the Bhukia Gold Prospect, the intensity of gold mineralization can be linked with profusion of carbonate veining which appears to have been remobilized from QFR layers. Petrographic features reveal that apart from the dominant quartz and feldspar, the QFR layers also contain actinolite, scapolite, biotite, titanite and fine graphitic grains. In spite of deformation and significant remobilization, the main sulfide zone has retained the concordant relationship with the lithological contacts (Golani, 1996).

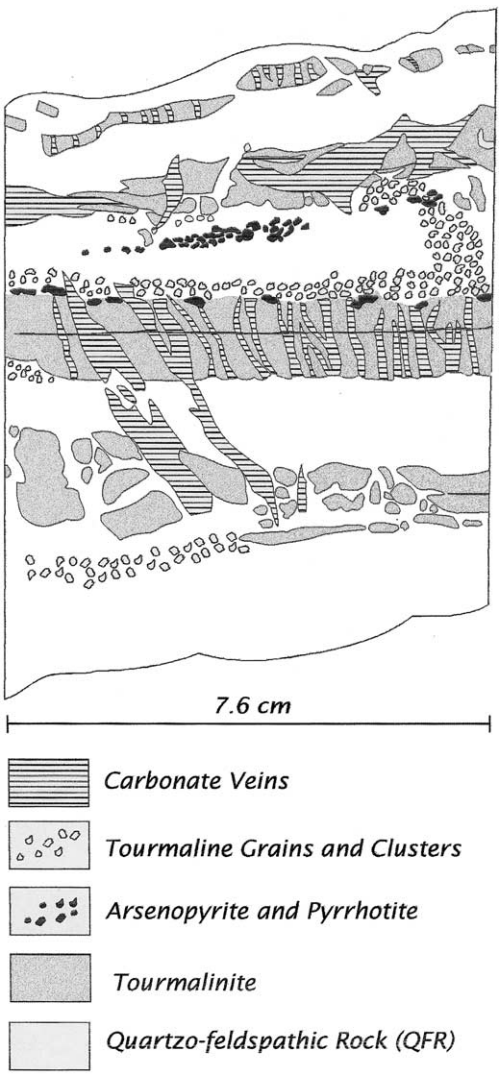

Fig. 5. Right side up sketch of a core cutting from eastern part of the Bhukia Gold Prospect illustrating the relationship between QFR–tourmalinite–arsenopyrite and carbonate veining.

Microprobe data indicate a high purity of gold (Golani et al., 1999) with fineness ranging from 922 to 995 (mean 963). Higher abundance levels of Co and Ni are characteristic of lollingite, which is the most favored residence of gold grains. Preliminary estimates from arsenopyrite composition and mineralogy of gold bearing ore assemblage, represented by arsenopyrite-lollingite and pyrrhotite, indicate a high temperature for the ore, attained probably during thermal metamorphism that was effected by some unexposed intrusion (Golani et al., 1999). High temperature of sulfide assemblage is also corroborated by the absence of pyrite (cf. Plimer, 1977).

5. Stable isotopes

5.1. Analytical methods and results

Representative samples of Bhukia carbonate (whole rock) and sulfide mineral separates were analyzed for C–O and S isotopic ratios, respectively. For C and O isotopic determinations, powdered samples were treated with 100% H_3PO_4 at 25 °C to release the CO_2 (McCrea 1950). More than 72 h was allowed to ensure complete reaction of slow reacting dolomite and to eliminate any isotopic fractionation effects. The $\delta^{13}C$ and $\delta^{18}O$ values were measured on cryogenically cleaned CO_2 (Craig, 1957) in a triple collector SIRA II mass spectrometer at NEG LABISE, Federal University of Pernambuco, Recife (Brazil). Borborema Skarn Calcite (BSC), calibrated against international standards, was used as the reference gas and reproducibility of measurements was better than $\pm 0.1‰$, in general. The values obtained for NBS-20 (as unknown) in a separate run against BSC yielded $\delta^{13}C = -1.05‰_{V\text{-}PBD}$, and $\delta^{18}O = -4.22‰_{V\text{-}PDB}$. These are in close agreement with the values reported by the US National Bureau of Standards (-1.06 and $-4.14‰$, respectively). The C and O isotopic compositions

Table 3
S-isotopic composition of sulfide mineral separates from Bhukia rocks

Sample	Mineral	$\delta^{34}S‰_{CDT}$
MB/18/16	Pyrrhotite	11.0
MB/18/32	Arsenopyrite	11.4
MB/18/159	Arsenopyrite	11.2
MB/18162	Arsenopyrite	11.3
MB/18/208	Arsenopyrite	12.8
MB/27/5	Arsenopyrite	12.8
MB/27/6	Arsenopyrite	12.7
MB/27/68	Pyrrhotite	10.5

are presented in Table 1 as standard ‰ deviation with reference to V-PDB and V-SMOW, respectively. S-isotopic analysis was performed on arsenopyrite and pyrrhoite mineral separates. Sulfur-dioxide was produced from sulfide separates using standard combustion procedures (after Robinson and Kusakabe, 1975) and isotopically analyzed on a VG SIRA II mass spectrometer at Scottish Universities Research and Reactor Center, Glassgow (Scotland). Precision and accuracy are better than $\pm 0.2‰$ (at σ) and all data are reported as ‰ deviations with reference to CDT (Table 3).

5.2. S-isotopes

S-isotope analyses performed on arsenopyrite and pyrrhotite mineral separates have yielded almost homogenous $\delta^{34}S$ values, ranging from $+10.5$ to $+12.8‰_{CDT}$ (Table 3). These values are much higher than the $+5‰$ level, generally ascribed upper limit for magmatic sulfur (e.g. Nielsen, 1979). The narrow spread of $\delta^{34}S$ values of Bhukia sulfides is also inconsistent with the biogenic accumulations which generally show strong and nonsystematic variations (Melezhik et al., 1998; see also Nielsen, 1979). The $\delta^{34}S$ values for biogenic sulfides could be as low as $-30.6‰_{CDT}$, as reported from the ~ 2.3 Ga old sulfides of Timeball Hill Formation of the Transvaal Supergroup in South Africa (Cameron, 1983). In contrast, the limited range of $\delta^{34}S$ values of Bhukia sulfides is consistent with abiogenic deposition in a hypersaline to evaporitic environment which show enrichment in the heavier isotopic component of sulfur (Holser, 1977). Our $\delta^{34}S$ values ($+10.5$ to $+12.8‰$) are closely comparable to the S-isotopic composition of pyrite ($\delta^{34}S = 10.5–13.7‰$) associated with boron ores of Liodong Peninsula in China (Zhang, 1988), interpreted as metamorphosed evaporates (Peng and Palmer, 1995; Jiang et al., 1997).

5.3. C–O isotopes

Bhukia carbonates are characterized by $\delta^{18}O$ values ranging from $+15.3$ to $+26‰_{V\text{-}SMOW}$ which are slightly depleted when compared with the Palaeoproterozoic carbonate compositions (Schidlowski et al., 1975; Sathyanarayan et al., 1987). The C- and O-isotopic compositions are non-correlative with each other, as seen in the $\delta^{18}O$–$\delta^{13}C$ diagram (Fig. 6), however, the $\delta^{13}C$ values show a bimodal distribution with total data ranging from -4.1 to $+0.3‰_{V\text{-}PDB}$ (Table 1), allowing the discrimination into two groups (Fields I and II, see Fig. 6) each with closely similar C-isotopic ratios. A narrow range of C-isotopic ratios for Field II (Fig. 6) carbonates indicates unmodified compositions while a spread in O-isotopic ratios indicates slightly modified $\delta^{18}O$ values as a result of evaporative conditions (trend A) and high temperature burial and/or exposure to meteoric waters (trend B, see Burdett et al., 1990). The Field I carbonates with similar C- and O-isotopic ratios best approximate the unmodified marine sedimentary carbonate signatures (Burdett et al., 1990; see also Sathyanarayan et al., 1987) and closely compare with the Aravalli stromatolitic phosphate-bearing carbonates of Udaipur area (Banerjee et al., 1986). In the absence of any evidence of algal activity in the Bhukia area, the Field II representing 'lighter' carbon component (mean value $-3.1‰_{V\text{-}PDB}$) may either indicate decarbonation due to thermal metamorphism or a mantle-derived carbon component. Despite evidence of high-grade metamorphism, such as development of spherulitic graphite in arsenopyrite (Golani et al., 1999) and occurrence of rare fine graphitic flakes in QFR,

we are inclined to interpret our negative $\delta^{13}C$ values in terms of mantle affinity as they can be considered unmodified being homogeneous. Moreover, the $\delta^{18}O$ values (mean $+20.6‰_{V\text{-}SMOW}$) are close to the low-grade Proterozoic evaporitic carbonates of Lomagundi (+22.6‰ see Schidlowski et al., 1975) and Karnataka (+21.6‰ see Sathyanarayan et al., 1987). Thermal decarbonation would normally result in lowering of both $^{13}C/^{12}C$ and $^{18}O/^{16}O$ ratios (Shieh and Taylor, 1969; Bottinga, 1969). It is clear from the foregoing sections that the host-rocks of gold-sulfide mineralization were deposited in a hypersaline to evaporitic environment. It is also well-known that the Proterozoic carbonates in evaporitic setting are invariably enriched in the heavier carbon such as Lomagundi carbonates (mean $\delta^{13}C + 8.2 \pm 2.6‰_{V\text{-}PDB}$) of Zimbabwe (Schidlowski et al., 1976); Badami and Bhima Groups (mean $+ 3.4 \pm 0.5‰$) from south India (Sathyanarayan et al., 1987); Beckspring dolomite (mean + 3‰) from eastern California (Tucker, 1983). The Bhukia Field II C-isotopic signatures ($-3.1‰$) are in sharp contrast to above carbonates as well as highly ^{13}C-enriched ($\delta^{13}C + 6.5$ to $+11‰_{V\text{-}PDB}$) Paleoproterozoic Aravalli carbonates of Udaipur region (Sreenivas et al., 2001; Maheshwari et al., 1999). Any association of Bhukia carbonates (Field II, Fig. 6) with the 'negative shift' (following each of the three Palaeoproterozoic positive excursions) is precluded for being significantly below 0‰ (Melezhik et al., 1999). The ^{13}C-depleted Bhukia carbonates appear to be consistent with the Archaean greenstone-hosted gold deposits (Groves et al., 1988). The $\delta^{13}C$ negative values, can therefore, be attributed to a mantle source. This mantle flux emanated through palaeofaults either from the granite–greenstone substratum, the remnants of which have been reported from this region by Sahoo and Mathur (1991), Upadhyaya et al. (1992) or through the coeval carbonatite magmatism (2.27 Ga see Schleicher et al., 1997) in the adjacent areas.

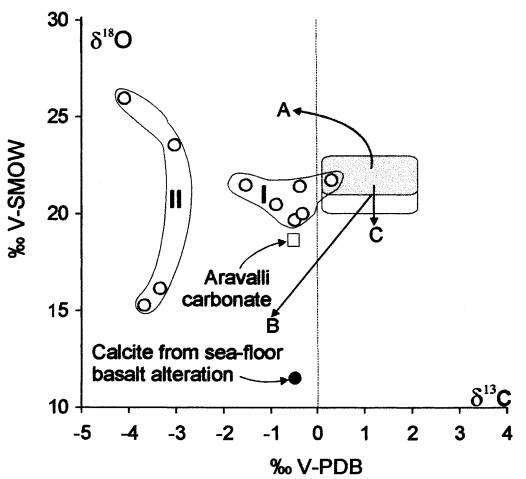

Fig. 6. Relationship between C and O isotopes in Bhukia carbonates in the conventional $\delta^{18}O$–$\delta^{13}C$ cross-plot showing discrimination of data into two fields. Field I carbonates show normal sedimentary values while Field II are close to mantle values. Shaded box (Burdett et al., 1990) represents the average sedimentary carbonate composition; alteration trends resulting from evaporitic modifications (A), high-temperature burial and/or exposure to meteoric waters (B) and weathering (C) are also shown (see Burdett et al., 1990). Average composition of Aravalli carbonates of Jhamarkotra Formation (Banerjee et al., 1986) and calcite from sea-floor basalt alteration (Groves et al., 1988) are also plotted for comparison.

6. Source of light carbon and origin of hypersaline conditions

We have two sets of data to constrain the origin of the hydrothermal fluids. These are the lighter carbon enriched isotopic composition of the carbonates, and the hypersaline to evaporitic depositional environment of host rocks with fairly extensive hydrothermal haloes, represented mainly by iron sulfide. The heavier carbon depleted C-isotopic ratios indicate a deep crustal or mantle affinity, comparable to the Late Archaean gold deposits of granite-greenstone belts of Australia and Canada, notably the Hollinger–Mclntyre ($-3.1‰ \pm 1.3_{V\text{-}PDB}$) and Golden Mile ($-3.4‰ \pm 0.40$) deposits (Groves et al., 1988). We are also inclined to attribute the significantly negative $\delta^{13}C$ values of Bhukia carbonates to a mantle source on the strength of coeval (2.27 Ga) carbonatite magmatism in the region, reported from Newania (Schleicher et al., 1997). Newania carbonatite rocks are also variable in $\delta^{13}C$ signa-

tures (Gruau et al., 1995; Pandit and Golani, 2001) and have yielded anomalously high gold values (Golani and Pandit, 1999), allowing a distinct possibility of their genetic relationship with heavier carbon depleted Bhukia carbonates. High TiO_2 content for Bhukia rocks coupled with the feeble radioactivity displayed by minerals like titanite, epidote and opaques further indicate the role of carbonatite-alkaline magmatism during the development of host rocks for gold mineralization. Simultaneous consideration of carbon and sulfur isotopic data has led us to interpret the sulfide deposition in an evaporitic environment with mantellic flux of carbon through deep palaeofaults. High gravity structures (see Reddy and Ramakrishana, 1988) and the fracture-riddled auriferous tract underlying the Bhukia area (D.J. Das Gupta, personal communication) afford the necessary tectonic setting for upward movement of the mantle-carbon bearing hydrothermal fluids. The mantle-carbon may have been channeled through such deep-seated, rift-related faults in the Aravalli basin, coincident with the deposition of Bhukia sequence (cf. Newton, 1990).

The host rocks for gold-sulfide mineralization are characterized by higher Na, B and Mg concentrations ($\pm$ radiogenic elements) and a lower K abundance. Higher Na content can be attributed either to the presence of degrading acid volcanic rocks in the sequence or to a deeper source related to major fractures (Plimer, 1977, 1985). Absence of acid volcanic rocks and very low abundance levels of Zn and particularly Pb, preclude any major role of shallow level acid volcanic system during evolution of the Bhukia sequence. Likewise, the supply of metasomatic Na from any unexposed granitoid is not favored on the strength of evidence such as well-banded nature of QFR, enhanced concentration of Na in carbonates coupled with development of sodic species of tourmaline (elbaite-dravite series) and chemical purity of the albite.

We attribute higher soda and boron concentrations as well as some radioactive elements of the host-rock to a deeper source, cogenetic with the mantellic carbon. There are several reports of occurrence of sodic rocks, the albitites, in northeastern and central Rajasthan, emplaced along major lineaments (Ray, 1990; Fareeduddin and Bose, 1992). Widespread Na-metasomatism associated with lineaments has also been recorded in several areas of southeastern Rajasthan (Ametha and Das Gupta, 1996). In most of these occurrences the soda-rich rocks and albitites occur as dykes related to major fractures. However, in case of Bhukia area, Na and B were probably exhaled into the depositional basin through palaeofaults. Enhanced concentration of such elements led to the hypersalinity, which eventually developed into evaporitic conditions. The sulfur isotope data ($\delta^{34}S$ between $+10.5$ and $+12.8‰_{CDT}$) strongly support abiogenic hypersaline conditions. The pulses of exhalation were followed by quiescence, which allowed dispersal of Na–B in the depositional basin. This is reflected by the consistently very low Fe/Al ratio (0.17) against high ratios (mean 38.5) normally reported for submarine hydrothermal fluids (e.g. Guaymas Basin-Von Damm et al., 1985). Association of albite-rich sediments (QFR) with tourmaline underlines significant role of terrigenous sediments in supplying Al as alumino-silicates are scarce in the sea-floor hydrothermal precipitates (see Boström et al., 1969). Ore-gangue rip-off fragments in well-banded QFR, impersistent laminae of tourmaline, and banded sulfide ore suggest that hydrothermal fluids spasmodically emptied their fluxes into local exhalative sites along deep rift-related faults within a shallow hypersaline basin. The depositional environment of Bhukia is comparable, to some extent, with the modern lakes along the East African rift-system where Tiercelin et al. (1989) have discovered hydrothermal activity in sublacustrine conditions with precipitation of pyrite. Iron sulfides have been the main sulfide facies in rift-related east African lakes as has been the case in Bhukia. The lighter C-isotopic component, higher abundance of Na, B, Au and some radiogenic elements represent the lower crust–mantle components; contained in the carbonate–QFR–tourmaline rich lithofacies of evaporitic affinity in the Bhukia Gold Prospect.

Acknowledgements

We gratefully acknowledge Eric Marcoux of BRGM (France) for discussion and review of the earlier draft of the manuscript. We are thankful to Dr M.E. Barley and Dr S.Y. Jiang for critical reviews and useful comments on the earlier version of the manuscript that have greatly improved it. P.R. Golani is thankful to Dr Davay, S. Chattopadhyaya, A.K. Grover and R.G. Verma of Geological Survey of India for fruitful discussion on Bhukia Gold Prospect. M.K. Pandit is grateful to CNPq, Brazil for grant of visiting fellowship and to University of Rajasthan for sabbatical leave. We are thankful to Roberta Galba Brasilino of Federal University of Pernambuco, Brazil for drafting the figures and to Gilsa Maria de Santana and Vilma Sobral for help in C–O isotopic analyses. A.B. Roy wishes to thank AICTE for financial assistance in form of Emeritus Fellowship. This is the contribution Number 183 of NEG LABISE.

References

Ametha, S.S., Das Gupta, D.J., 1996. Observations on soda-rich rocks and their association with copper mineralization in Bhilwara and Delhi metallotect, Rajasthan. National seminar on mineralization in the western Indian Craton. Delhi University, p. 34 Abstract.

Banerjee, D.M., 1971. Precambrian stromatolitic phosphorites of Udaipur, Rajasthan, India. Bull. Geol. Soc. Am. 82, 2319–2330.

Banerjee, D.M., Schidlowski, M., Arneth, D., 1986. Genesis of Upper Proterozoic Cambrian phosphorite deposits of India, isotopic inferences from carbonate fluorapatite, carbonate and organic carbon. Precambrian Res. 33, 239–253.

Boström, K., Peterson, M.N.A., Joensuu, O., Fisher, D.E., 1969. Aluminium-poor ferromanganoan sediments on active ocean ridges. J. Geophys. Res. 74, 3261–3270.

Bottinga, Y., 1969. Calculated fractionation factors for carbon and hydrogen isotope exchange in the system calcite–carbon dioxide–graphite–methane–hydrogen–water vapor. Geochim. Cosmochim. Acta 33, 49–64.

Burdett, J.W., Grotzinger, J.P., Arthur, M.A., 1990. Did major changes in the stable isotopic composition of seawater occur. Geology 26, 875–878.

Cameron, E.M., 1983. Evidence from early Proterozoic anhydrite for sulfur partitioning in Precambrian oceans. Nature 304, 54–56.

Cook, N.D.J., Ashley, P.M., 1992. Metaevaporite sequence, exhalative chemical sediments and associated rocks in the Proterozoic Willyama Supergroup, south Australia: Implications of metallogenesis. Precambrian Res. 56, 211–226.

Craig, H., 1957. Isotope standards for carbon and oxygen and correction factors for mass spectrometry analysis of carbon dioxide. Geochim. Cosmochim. Acta 12, 133–149.

Fareeduddin, Bose, U., 1992. A new occurrence of albitite dyke near Arath, Nagaur district, Rajasthan. Curr. Sci. 62, 635–636.

Fiermans, M., Paepe, P.D., 1982. Genesis of tourmalinites from Belgium: petrographic and chemical evidence. Mineralog. Mag. 46, 95–102.

Golani, P.R., 1996. Lithologic and structural controls on Sulfide–Gold Mineralization in Bhukia–Jagpura Area, Banswara District, Rajasthan. Workshop on Gold Resources of India, Geological Society of India. National Geophysical Research Institute, Hyderabad, p. 161 Abstract.

Golani, P.R., Pandit, M.K., 1999. Evidence of epithermal activity and gold mineralization in Newania Carbonatite, Udaipur, Rajasthan. J. Geol. Soc. India 64, 251–257.

Golani, P.R., Rajawat, R.S., Pant, N.C., Rao, M.S., 1999. Mineralogy of gold and associated alloys in sulfides of Bhukia Gold Prospect in southeastern Rajasthan, western India. J. Geol. Soc. India 64, 121–128.

Gopalan, K., Macdougall, J.D., Roy, A.B., Murali, A.V., 1990. Sm–Nd evidence for 3.3 Ga old rocks in Rajasthan, northwestern India. Precambrian Res. 48, 287–297.

Grover, A.K., Verma, R.G., 1993. Gold mineralization in Precambrian (Bhukia area) of southeastern Rajasthan—A new discovery. J. Geol. Soc. India 42, 281–288.

Groves, D.I., Golding, S.D., Rock, N.M.S., Barley, M.E., McNaughton, N.J., 1988. Archaean carbon reservoirs and their relevance to the fluid source for gold deposits. Nature 331, 254–257.

Gruau, G., Petibon, C., Viladkar, S., Fourcade, S., Bernard-Griffiths, J., Mace, J., 1995. Extreme isotopic signatures in carbonatites from Newania, Rajasthan. Terra Nova 7 (Suppl. 1), 336 Abstract.

Henry, D.J., Guidotti, C.V., 1985. Tourmaline as a petrogenetic indicator mineral: an example from staurolite grade metapelites of NW Maine. Am. Mineral. 70, 1–15.

Heron, A.M., 1953. The Geology of Central Rajputana. Geol. Surv. India Mem. 79, 1–389.

Holser, W.T., 1977. Catastrophic chemical events in the history of oceans. Nature 267, 403–408.

Jiang, S.Y., Palmer, M.R., Peng, Q.M., Yang, J.H., 1997. Chemical and stable isotopic compositions of Proterozoic metamorphosed evaporites and associated tourmalinites from the Houxinaya borate deposits, eastern Lixoning, China. Chem. Geol. 135, 189–211.

Kastner, M., Siever, R., 1979. Low temperature feldspars in sedimentary rocks. Am. J. Sci. 279, 435–479.

Kemp, S., Degens, E.T., 1985. An early soda ocean. Chem. Geol. 53, 95–108.

Land, L.S., Hoops, G.K., 1973. Sodium in carbonate sediments and rocks: a possible index of salinity of diagenetic solutions. J. Sediment. Petrol. 43, 614–617.

Leake, B.E., Singh, D., 1986. The Delaney Dome Formation, Connemara, W. Ireland and the distinction of Ortho-and Para-quartzo feldspathic rocks. Mineral. Mag. 50, 205–215.

Macdougall, J.D., Willis, R., Lugmair, G.W., Gopalan, K., Roy, A.B., 1984. The Aravalli Sequence of Rajasthan, India: A Precambrian Continental Margin. Proceedings-Workshop on the Early Earth: The interval from Accretion to the Older Archaean. Lunar Planetary Institute, Houston, Texas, pp. 55–56 Abstract.

Maheshwari, A., Sial, A.N., Chittora, V.K., 1999. High $\delta^{13}C$ Palaeoproterozic carbonates from the Aravalli Supergroup, western India. Intl. Geol. Rev. 41, 949–954.

McCrea, J.M., 1950. On the isotopic chemistry of carbonates and a palaeotemperature scale. J. Chem. Phy. 18, 849–857.

Melezhik, V.A., Grinenko, L.N., Fallick, A.E., 1998. 2000-Ma sulfide concretions from the 'Productive' Formation of the Pechenga Greenstone Belt, NW Russia: genetic history based on morphological and isotopic evidence. Chem. Geol. 148, 61–94.

Melezhik, V.A., Fallick, A.E., Medvedev, P.V., Makarikhin, V.V., 1999. Extreme $\delta^{13}C_{carb}$ enrichment in ca. 2.0 Ga magnesite–stromatolite–dolomite–'red beds' association in a global context: a case for the world-wide signal enhanced by a local environment. Earth Sci. Rev. 48, 71–120.

Moine, B., Sauvan, P., Jorousse, J., 1981. Geochemistry of Evaporite–Bearing Series: a tentative guide for the identification of metaevapontes. Contrib. Mineral. Petrol. 76, 401–412.

Naha, K., Roy, A.B., 1983. The problem of the Precambrian basement in Rajasthan. Precambrian Res. 19, 217–223.

Neudert, M.K., Russell, R.E., 1981. Shallow water hypersaline features from the middle Proterozoic Mt. Isa sequence. Nature 293, 284–286.

Newton, R.C., 1990. Fluids and shear zones in the deep crust. Tectonophysics 162, 21–37.

Nielsen, H., 1979. Sulfur isotopes. In: Jager, E., Hunziker, J. (Eds.), Lectures in Isotope Geology. Springer, Berlin, pp. 283–312.

Paliwal, B.S., 1998. The Aravallian fluvial sequence of Udaipur City, India: an excellent example of well preserved sedimentary structures in complexly deformed Precambrian metasediments. In: Paliwal, B.S. (Ed.), The Indian Precambrian. Scientific Publishers, Jodhpur, India, pp. 142–158.

Pandit, M.K., Golani, P.R., 2001. Reappraisal of the petrologic status of Newania 'carbonatite' of Rajasthan, western India. J. Asian Earth Sci. 19, 305–310.

Peng, Q.M., Palmer, M.R., 1995. The Palaeoproterozoic boron deposits in eastern Lianing, China: a metamorphosed evaporite. Precambrian Res. 72, 185–197.

Plimer, I.R., 1977. The origin of albite-rich rocks enclosing the cobaltian pyrite deposit at Thackaringa, N.S.W. Australia. Mineralium. Dep. 12, 175–187.

Plimer, I.R., 1985. Broken Hill Pb–Zn–Ag deposit-a product of mantle metasomatism. Mineralium. Dep. 20, 147–153.

Ray, S.K., 1990. The albitite line of northern Rajasthan—a fossil intracontinental rift zone. J. Geol. Soc. India 36, 413–423.

Reddy, A.G.B., Ramakrishana, T.S., 1988. Bouguer Gravity Atlas of western Indian (Rajasthan–Gujarat) Shield. Geol. Surv. India Publication.

Robinson, B.W., Kusakabe, M., 1975. Quantitative preparation of sulfur dioxide for 34s/32s analyses from sulfides by combustion with cuprous oxide. Analyt. Chem. 47, 1179–1181.

Roy, A.B., Paliwal, B.S., 1981. Evolution of lower Proterozoic epicontinental sediments: stromatolite bearing Aravalli rocks of Udaipur, Rajasthan, India. Precambrian Res. 14, 49–74.

Roy, A.B., Kröner, A., 1996. Single zircon evaporation ages constraining the growth of Archaean Aravalli Craton, northwestern indian shield. Geol. Mag. 133, 333–342.

Roy, A.B., Kataria, P., 1999. Precambrian geology of the Aravalli Mountain and neighbourhood: analytical update of recent studies. In: Kataria, P. (Ed.), Proceeding of Seminar on Geology of Rajasthan: Status and Perspective. MLS University, Udaipur, pp. 1–56.

Roy, A.B., Paliwal, B.S., Shekhawat, S.S., Nagori, D.K., Golani, P.R., Bejarniya, B.R., 1988. Stratigraphy of the Aravalli Supergroup in the type area. In: Roy, A.B. (Ed.), Precambrian of the Aravalli Mountain Range. Geol. Soc. India Mem. 7, 121–138.

Sahoo, K.C., Mathur, A.K., 1991. On the occurrence of Sargur type banded iron formation in Banded Gneissis Complex of south Rajasthan. J. Geol. Soc. India 38, 299–302.

Sathyanarayan, S., Arneth, J.D., Schidlowski, M., 1987. Stable isotope geochemistry of sedimentary carbonates from the Proterozoic Kaladgi, Badami and Bhima Groups, Karnataka, India. Precambrian Res. 37, 147–156.

Schidlowski, M., Eichman, R., Junge, C.E., 1975. Precambrian sedimentary carbonates: carbon and oxygen isotope geochemistry and implications for the terrestrial oxygen budget. Precambrian Res. 2, 1–69.

Schidlowski, M., Eichman, R., Junge, C.E., 1976. Carbon isotope geochemistry of the Precambrian Lomagundi carbonate province. Rhodesia. Geochem. Cosmochim. Acta 40, 449–455.

Shieh, Y.N., Taylor, H.P., 1969. Oxygen and carbon isotope studies of contact metamorphism of carbonate rocks. J. Petrol. 10, 307–331.

Schleicher, H., Todt, W., Viladkar, S.G., Schmidt, F., 1997. Pb/Pb age determinations on the Newania and Sevattur carbonatites of India: evidence of multi-stage histories. Chem. Geol. 140, 261–273.

Schwartz, M.O., 1992. Geochemical criteria for distinguishing magmatic and metasomatic albite-enrichment in granitoids-examples from the Ta–Li granite Yichun (China) and Sn–W deposit Tikus (Indonesia). Mineralium. Dep. 27, 101–108.

Serdyuchenko, D.P., 1975. Some Precambrian scapolite bearing rocks evolved from evaporites. Lithos 8, 1–7.

Sreenivas, B., Sharma, S.D., Kumar, B., Patil, J.D., Roy, A.B., Srinivasan, R., 2001. Positive $\delta^{13}C$ excursion in carbonate and organic fractions from the Palaeoproterozoic Aravalli Supergroup, Northwestern India. Precambrian Res. 106, 277–290.

Tiercelin, J.J., Thouin, C., Kalala, T., Mondeguer, A., 1989. Discovery of sublacustrine hydrothermal activity and associated massive sulfides and hydrocarbons in the north Tanganyika trough, East African Rift. Geology 17, 1053–1056.

Tucker, M.E., 1983. Diagenesis, geochemistry and origin of a Precambrian dolomite: The Beck Spring dolomite of eastern California. J. Sed. Petrol. 53, 1097–1119.

Upadhyaya, R., Sharma, B.L. Jr, Sharma, B.L. Sr, Roy, A.B., 1992. Remnants of greenstone sequence from the Archaean rocks of Rajasthan. Curr. Sci. 62, 87–92.

Vinogradov, A., Tugarinor, A., Zhykov, C., Stapninkova, N., Bibilova, E., Khorre, K., 1964. Geochronology of Indian Precambrian. Proc. 22nd Int. Geol. Cong. New Delhi 10, 553–567.

Von Damm, K.L., Edmond, J.M., Measures, C.I., Grant, B., 1985. Chemistry of submarine hydrothermal solutions at Guaymas Basin, Gulf of California. Geochim. Cosmochim. Acta 49, 2221–2237.

Wiedenbeck, M., Goswami, I.N., Roy, A.B., 1996. Stabilization of the Aravalli Craton of Northwestern India at 2.5 Ga: an ion microprobe zircon study. Chem. Geol. 129, 325–340.

Zhang, S., 1988. Early Proterozoic tectonic styles and associated mineral deposits of the North China platform. Precambrian Res. 39, 147–156.